0026-895X/95/010131-09$3.00/0

MOLECULAR PHARMACOLOGY, 48:131–139 (1995).

ω-Grammotoxin SIA Blocks Multiple, Voltage-Gated, Ca^{2+} Channel Subtypes in Cultured Rat Hippocampal Neurons

TIMOTHY M. PISER, RICHARD A. LAMPE, RICHARD A. KEITH, and STANLEY A. THAYER

Department of Pharmacology, University of Minnesota Medical School, Minneapolis, Minnesota 55455 (T.M.P., S.A.T.), and Department of Pharmacology, Zeneca Pharmaceuticals Group, Zeneca Inc., Wilmington, Delaware 19897 (R.A.L., R.A.K.)

Received February 17, 1995; Accepted April 24, 1995

SUMMARY

ω-Grammotoxin SIA is a peptide isolated from tarantula venom on the basis of its ability to block the voltage-gated Ca^{2+} channels that mediate glutamate release. To determine the Ca^{2+} channel subtype selectivity of ω-grammotoxin SIA, whole-cell Ba^{2+} current (I_{Ba}) was measured in cultured rat hippocampal neurons. Selective Ca^{2+} channel blockers were used to identify components of I_{Ba} mediated by Ca^{2+} channel subtypes. ω-Agatoxin IVA at 30 nM, 1 μM ω-conotoxin GVIA, and 3 μM ω-conotoxin MVIIC, applied consecutively, each elicited a fractional increase in the cumulative block of I_{Ba}, identifying components of I_{Ba} mediated by P-, N-, and Q-type calcium channels. ω-Grammotoxin at 1 μM, a maximally effective concentration, blocked 52% of I_{Ba}. ω-Conotoxin MVIIC and the combination of ω-conotoxin GVIA and micromolar ω-agatoxin IVA blocked 52% and 54% of I_{Ba}, respectively, and block of I_{Ba} by ω-grammotoxin SIA was mutually occlusive of block of I_{Ba} by either treatment, both of which block N-, P-, and Q-type Ca^{2+} channels. The L channel blocker nimodipine produced identical block of I_{Ba} in the presence and absence of ω-grammotoxin SIA. These results indicate that ω-grammotoxin SIA blocks N-, P-, and Q-type but not L-type voltage-gated calcium channels. Block of I_{Ba} by ω-grammotoxin SIA was faster in onset and less sensitive to external divalent cation concentrations than was block by ω-conotoxin MVIIC, and it was rapidly and substantially reversible. Rapid onset, relative insensitivity to divalent cation concentrations, and reversibility render ω-grammotoxin SIA a useful tool for inhibition of neuronal voltage-gated Ca^{2+} channels.

Voltage-gated Ca^{2+} channels convert changes in membrane potential into elevations in cytosolic Ca^{2+}, a biochemical trigger for such diverse processes as neurotransmitter release (1), regulation of neuronal excitability (2), and activation of transcription (3). These channels have been classified into several subtypes on the basis of distinct biophysical properties and selective pharmacology (4–8). Some biophysical and pharmacological properties of native channel subtypes match those of cloned Ca^{2+} channel α1 subunits (9–11).

In this report, we use natural toxins to identify Ca^{2+} channel subtypes in cultured rat hippocampal neurons. Natural toxins have become indispensable tools for the study of voltage-gated Ca^{2+} channels. Three of the four pharmacologically identified, high voltage-activated, Ca^{2+} channels are defined by their sensitivity to block by peptide toxins isolated from natural venoms (6–8, 12). ω-CgTx GVIA, isolated from the venom of the marine snail *Conus geographus*, was the first peptide toxin used to pharmacologically identify a Ca^{2+} channel subtype (6, 12). Low micromolar concentrations of ω-CgTx GVIA completely, selectively, and irreversibly block mammalian N-type Ca^{2+} channels (6, 13, 14), and ω-CgTx GVIA block demonstrates a role for N channels in the release of several neurotransmitters (11), including glutamate (15–18). P-type Ca^{2+} channels are completely blocked by 60–200 nM ω-Aga IVA, a peptide isolated from the venom of the funnel-web spider, *Agenelopsis aperta* (7). P channels also mediate the release of several neurotransmitters (11), including glutamate (16, 18–20).

In several types of neurons, Ca^{2+} channel current not blocked by dihydropyridine L-type Ca^{2+} channel blockers, the N channel blocker ω-CgTx GVIA, or P channel-selective concentrations of ω-Aga IVA suggests the existence of voltage-gated Ca^{2+} channels that are not L-, N-, or P-type (21). Randall and Tsien (8) have identified five components of Ca^{2+} channel current in cultured cerebellar granule neurons. In addition to L- and N-type currents, two current components that were differentially sensitive to ω-Aga IVA and exhibited dissimilar inactivation kinetics were clearly distinguished. One component was blocked by ω-Aga IVA with a K_d of 1 nM and showed little inactivation during a depolarizing

This work was supported by grants from the National Institutes of Health (DA07304) and the National Science Foundation (IBN9412654). T.M.P. was supported by the National Institute on Drug Abuse (Grant T32-DA07234).

ABBREVIATIONS: ω-CgTx GVIA, ω-conotoxin GVIA; ω-GsTx SIA, ω-grammotoxin SIA; ω-CmTx MVIIC, ω-conotoxin MVIIC; ω-Aga IVA, ω-agatoxin IVA; I_{Ba}, barium current; TEA, tetraethylammonium; HEPES, 4-(2-hydroxyethyl)-1-piperazineethanesulfonic acid; BAPTA, 1,2-bis(2-aminophenoxy)ethane-*N,N,N′,N′*-tetraacetic acid.

test pulse, neatly fitting the known characteristics of P-type current. The second component was blocked by ω-Aga IVA with a K_d of 89 nM, exhibited marked inactivation during a test pulse, and was designated Q-type current (8). Q-type current, like N- and P-type but not L-type current (22), was further shown to be blocked by ω-CmTx MVIIC (8), a toxin cloned from the marine snail *Conus magus*. Thus, Ca^{2+} channel current mediated by Q channels can be pharmacologically defined as being insensitive to ω-CgTx GVIA and P channel-selective concentrations of ω-Aga IVA but blocked either by micromolar concentrations of ω-Aga VIA or by ω-CmTx MVIIC. Clearly, care must be exercised when distinguishing between P- and Q-type currents, because no single agent is selective for either component. Nevertheless, a Q-type component of Ca^{2+} channel current has also been identified in acutely dissociated hippocampal CA3 neurons (23). Complete block by ω-CmTx MVIIC of glutamate synaptic transmission at the CA3-CA1 synapse in the hippocampus but only partial block by ω-CgTx GVIA, with no effect of P channel-selective concentrations of ω-Aga IVA, indicates that Q channels also mediate glutamate release (17). Clearly, peptide toxins are essential tools for the study of voltage-gated Ca^{2+} channels, and either a mixture of selective toxins or a relatively non-selective toxin such as ω-CmTx MVIIC may be required to pharmacologically eliminate release of neurotransmitter at many synapses.

ω-GsTx SIA is a peptide toxin purified from the venom of the tarantula spider, *Grammostola spatulata*, on the basis of its ability to block depolarization-evoked $^{45}Ca^{2+}$ influx in purified rat brain synaptosomes and depolarization-evoked D-[^{3}H]aspartate release from rat hippocampal slices (24). Block by ω-GsTx SIA of these indirect measures of Ca^{2+} channel activity suggests that ω-GsTx SIA blocks the voltage-gated Ca^{2+} channels that mediate glutamate release. Inhibition of synaptosomal $^{45}Ca^{2+}$ influx and hippocampal D-[^{3}H]aspartate release by ω-GsTx SIA overlaps with inhibition by ω-CgTx GVIA, ω-Aga IVA, and ω-CmTx MVIIC, suggesting that ω-GsTx SIA shares Ca^{2+} channel subtype specificity with characterized Ca^{2+} channel toxins. These results are consistent with the ability of each of these toxins to inhibit neurotransmitter release and neurotransmission at some synapses. ω-GsTx SIA appears not to block L channels; ω-GsTx SIA does not inhibit depolarization-evoked contraction of aorta (24) or prevent an increase in whole-cell Ca^{2+} current elicited by the L channel agonist Bay K8644 (25). The present study further defines the Ca^{2+} channel subtype specificity of ω-GsTx SIA and describes properties of ω-GsTx SIA, in comparison with ω-CmTx MVIIC, that will render ω-GsTx SIA a useful tool for the study of voltage-gated Ca^{2+} channels and the cellular processes mediated by them.

Materials and Methods

Cell culture. Hippocampal neurons were grown in primary culture as described by Thayer *et al.* (26), with minor modifications. Briefly, hippocampi were dissected from the brains of Sprague-Dawley rat fetuses removed at gestational day 17 from maternal rats that had been asphyxiated with CO_2 and decapitated. Hippocampi were dissociated by trituration through multiple, increasingly constricted, glass Pasteur pipettes. The dissection and dissociation were done in a Ca^{2+}- and Mg^{2+}-free, HEPES-buffered, Hanks' solution containing 20 mM HEPES, 137 mM NaCl, 5 mM KCl, 0.4 mM KH_2PO_4, 0.6 mM $NaHPO_4$, 3 mM $NaHCO_3$, and 5.6 mM glucose, pH 7.4 with NaOH (osmolarity, 300 mOsm/kg). The resulting cell suspension was centrifuged at 1000 rpm for 10 min, the supernatant was removed, and the cells were resuspended in Dulbecco's modified Eagle's medium (Gibco) supplemented with 10% fetal bovine serum (Sigma). Cells were plated in six-well culture plates, at 50,000 cells/well, onto 25-mm round coverglasses that had been coated overnight with poly-D-lysine (0.1 mg/ml in borate buffer, pH 8.6; Sigma) and washed with water. Neurons were grown in a humidified atmosphere of 10% CO_2/90% air at 37°. Twenty-four to 72 hr after plating, the medium was exchanged for Dulbecco's modified Eagle's medium supplemented with 10% horse serum (Sigma), and 0.5 ml of the medium was exchanged every 7 days thereafter. Cells were grown in culture for 12–24 days.

Electrophysiology. Whole-cell recordings were obtained from cultured neurons using pipettes (3–5-MΩ resistance) pulled from borosilicate glass (Narashige) on a Sutter Instruments P-87 micropipette puller. Pipettes were filled with a solution containing 140 mM cesium methanesulfonate, 10 mM BAPTA, 10 mM HEPES, and 5 mM MgATP, pH 7.3 with CsOH; the osmolarity of the pipette solution was adjusted to 315 mOsm/kg with sucrose. Whole-cell recordings were established in a solution containing 133 mM NaCl, 2.5 mM KCl, 10 mM $CaCl_2$, 1 mM $MgCl_2$, 10 mM glucose, and 10 mM HEPES, pH 7.4 with NaOH. Experiments were conducted at room temperature (22°) in an external solution containing 143 mM TEA-Cl, 5 mM $BaCl_2$, 1 mM $MgCl_2$, 10 mM glucose, 10 mM HEPES, and 1 mg/ml bovine serum albumin, pH 7.4 with TEA-OH. For the experiments conducted with 10 mM external Ba^{2+}, the concentration of TEA-Cl was lowered to 136 mM. The osmolarity of all external solutions was adjusted to 325 mOsm/kg with sucrose. Solutions were applied by a gravity-fed superfusion system; exchange of solutions was complete within 1 min. With few exceptions, recordings were obtained in a static bath, and drugs were applied by perfusing the chamber with the appropriate solution for 60–100 sec. Drugs were applied until an apparent steady state block was achieved. In most experiments, 1 mM Cd^{2+} was applied at the end of the experiment for subtraction of leak currents from currents mediated by Ca^{2+} channels. ω-GsTx SIA was synthesized according to published methods (24). ω-GsTx SIA, ω-Aga IVA, ω-CmTx MVIIC (Bachem, Torrance, CA), and ω-CgTx GVIA (Sigma Chemical Co., St. Louis, MO) were stored at −20° as 5-μl aliquots in water, at 400 times the reported concentrations, and were thawed immediately before use. Nimodipine (Research Biochemicals, Natick, MA) was stored at −20° as a 10 mM stock solution in ethanol and was diluted immediately before use.

Whole-cell currents were recorded using an Axopatch 200A patch-clamp amplifier and the BASIC-FASTLAB interface system (INDEC Systems). Currents were filtered at 1 kHz (four-pole, Bessel, low-pass filter) and sampled every 200 μsec. Series resistance was compensated by 75–90% of the value required to eliminate the uncompensated capacity transient evoked by voltage steps from −80 to −90 mV. Voltage errors due to uncompensated series resistance did not exceed 4 mV. In all experiments, high-threshold Ca^{2+} channel currents were elicited every 20 sec by a 40-msec depolarizing pulse to a test potential of 0 mV from a holding potential of −80 mV. When rundown was apparent in the base-line period, the plot of peak current versus time during the base-line period was fit with a single-exponential equation and extrapolated to individual time points to obtain I_{max}. The maximal inward current measured at any point between the onset and offset of the test pulse was designated as peak current, I, for a given trace; this point always occurred within the first 10 msec of the 40-msec test pulse. Percentage inhibition was calculated with the formula $[(I_{max} - I)/I_{max}] \cdot 100$, in which I for a given treatment was determined by subtracting the average peak current of three sweeps obtained in the presence of Cd^{2+} from the average peak current of three sweeps obtained after inhibition of current had reached apparent equilibrium during that treatment. When sweeps in the presence of Cd^{2+} were not collected, leak currents were not subtracted. Displayed currents were not corrected for

leak. Values are given as mean ± standard error, and Student's *t* test was used to determine statistical significance.

Results

Whole-cell patch-clamp recordings were made with 139 fetal hippocampal neurons that had been maintained in primary culture for 12–24 days. Neurons were chosen that exhibited a pyramidal morphology, with dendritic branches extending from the vertices of a triangular cell body. Cells selected by these criteria probably include CA1 and CA3 hippocampal pyramidal cells and perhaps other hippocampal cell types. Internal and external monovalent cations were replaced with Cs^+ and TEA^+, respectively, and Ba^{2+} was provided as the charge carrier. Whole-cell I_{Ba}, elicited in these experiments by 40-msec test pulses from −80 mV to 0 mV applied at 20-sec intervals, was mediated by the activation of voltage-gated Ca^{2+} channels, as confirmed by the absence of inward current in the presence of 1 mM Cd^{2+}. We measured I_{Ba} to detect the effects of peptide toxins on voltage-gated Ca^{2+} channels.

ω-GsTx SIA and ω-CmTx MVIIC produced concentration-dependent inhibition of I_{Ba}. Fig. 1 illustrates the results of experiments designed to determine the concentrations of ω-GsTx SIA and ω-CmTx MVIIC that elicit maximal inhibition of I_{Ba}. In Fig. 1, A and C, peak inward current recorded during each voltage step is plotted versus time; Fig. 1, B and D, shows current records from the same experiments. In the experiment illustrated in Fig. 1, A and B, consecutive application of 0.03, 0.3, and 1 μM ω-GsTx SIA produced progressively greater cumulative inhibition of I_{Ba}; however, 3 μM ω-GsTx SIA had no further effect. In three experiments in which 1 μM and 3 μM ω-GsTx SIA were consecutively applied to the same cell, 1 μM ω-GsTx SIA blocked 65 ± 3% of I_{Ba}, whereas 3 μM blocked 66 ± 3% of I_{Ba}. Similarly, in the experiment illustrated in Fig. 1, C and D, consecutive application of 0.3, 1, and 3 μM ω-CmTx MVIIC produced progressively greater cumulative inhibition of I_{Ba}, and 10 μM ω-CmTx MVIIC had no further effect. ω-CmTx MVIIC at 3 μM and 10 μM inhibited 59 ± 2% and 63 ± 2% of I_{Ba}, respectively, when applied consecutively to the same cells (n = 4). Thus, 1 μM ω-GsTx SIA and 3 μM ω-CmTx MVIIC elicited the maximal inhibition of I_{Ba} produced by these toxins.

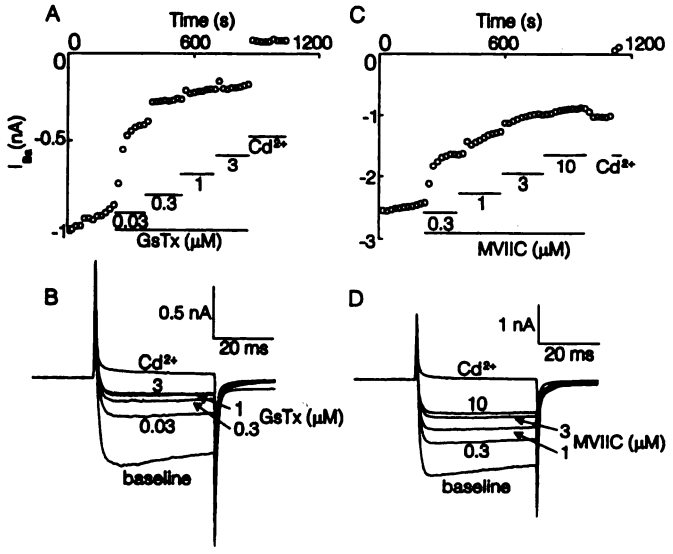

Fig. 1. Concentrations of 1 μM ω-GsTx SIA and 3 μM ω-CmTx MVIIC are maximally effective. A and C, Plots of peak current versus time, showing the effects of increasing concentrations of ω-GsTx SIA (*GsTx*) (A) and ω-CmTx MVIIC (*MVIIC*) (C). Drugs were applied as indicated (*bars*). B and D, Current records from the experiments shown in A and C, respectively. *Traces* are averages of three sweeps obtained during each treatment.

Maximally effective concentrations of ω-GsTx SIA or ω-CmTx MVIIC produced identical percentage block of I_{Ba}. When data were pooled across experiments, 1 μM ω-GsTx SIA blocked 51 ± 4% (n = 16), whereas 3 μM ω-CmTx MVIIC blocked 52 ± 4% (n = 11) of I_{Ba}. Percentage block produced by each toxin differed somewhat between sets of experiments; these discrepancies are potentially accounted for by underestimation of rundown in some cells and different levels of expression of Ca^{2+} channel subtypes in different hippocampal cell types (21). However, the overall identity in percentage block produced by the toxins suggests that ω-GsTx SIA and ω-CmTx MVIIC block the same component of I_{Ba}. To directly test this hypothesis, we conducted occlusion experiments in which maximally effective concentrations of either ω-GsTx SIA or ω-CmTx MVIIC were tested for the ability to occlude block of I_{Ba} by the other toxin. Fig. 2 illustrates the results of these experiments. In Fig. 2, A and C, peak inward current is plotted versus time, and current records from these experiments are shown in Fig. 2, B and D. In the experiment illustrated in Fig. 2, A and B, 1 μM ω-GsTx SIA produced 52% inhibition of I_{Ba}, and subsequent application of 3 μM ω-CmTx MVIIC in the presence of 1 μM ω-GsTx SIA produced 50% inhibition. In five similar experiments,

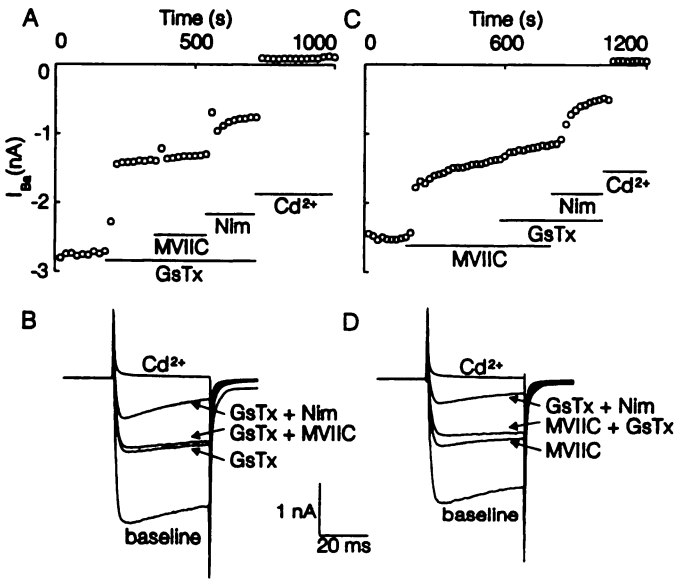

Fig. 2. ω-GsTx SIA and ω-CmTx MVIIC block identical components of Ca^{2+} channel current. A, Plot of peak current versus time, showing that block of I_{Ba} by ω-GsTx SIA (*GsTx*) (1 μM) occludes block by ω-CmTx MVIIC (*MVIIC*) (3 μM) but not block by nimodipine (*Nim*) (10 μM). C, Plot of peak current versus time, showing that block of I_{Ba} by ω-CmTx MVIIC occludes block by ω-GsTx SIA and that block by ω-GsTx SIA does not occlude block by nimodipine (same abbreviations and concentrations as in A). Drugs were applied as indicated (*bars*). B and D, Current records from the experiments in A and C, respectively. *Traces* are averages of three sweeps obtained during each treatment. *Scale bars* apply to both sets of currents.

ω-GsTx SIA alone blocked 46 ± 8% of I_{Ba}, whereas the combination of ω-CmTx MVIIC and ω-GsTx SIA produced no further effect (50 ± 8% inhibition). Thus, ω-CmTx MVIIC increased block of I_{Ba} by only 4.0 ± 1.1% over block elicited by ω-GsTx SIA, indicating that block of I_{Ba} by ω-GsTx SIA occluded block of I_{Ba} by ω-CmTx MVIIC. When the order of toxin application was reversed, the result was the same. In the experiment illustrated in Fig. 2, C and D, 3 μM ω-CmTx MVIIC blocked 31% of I_{Ba}, and subsequent application of 1 μM ω-GsTx SIA in the presence of ω-CmTx MVIIC increased block to 36% of I_{Ba}. In five similar experiments, ω-CmTx MVIIC alone blocked 48 ± 8% of I_{Ba}, whereas the combination of ω-GsTx SIA and ω-CmTx MVIIC had no further effect (51 ± 6% inhibition). Thus, ω-GsTx SIA increased block of I_{Ba} by only 3.4 ± 3.1% over block elicited by ω-CmTx MVIIC, indicating that block of I_{Ba} by ω-CmTx MVIIC occluded block of I_{Ba} by ω-GsTx SIA. The results of these occlusion experiments are consistent with the hypothesis that ω-GsTx SIA and ω-CmTx MVIIC block identical subpopulations of voltage-gated Ca^{2+} channels in cultured hippocampal neurons.

ω-CmTx MVIIC does not block L-type voltage-gated Ca^{2+} channels in acutely dissociated rat CA1 hippocampal neurons (22), and in the present study ω-GsTx SIA blocks the same component of Ca^{2+} channel current as does ω-CmTx MVIIC, suggesting that ω-GsTx SIA does not block L channels. Indeed, in the experiments illustrated in Fig. 2, a 10 μM concentration of the dihydropyridine L channel antagonist nimodipine produced a significant additional inhibition of I_{Ba} when applied in the presence of ω-GsTx SIA (from 52 ± 4% to 76 ± 4%, $p < 0.001$, $n = 11$). Furthermore, ω-GsTx SIA does not prevent an increase in whole-cell Ca^{2+} current elicited in rat dorsal root ganglion neurons by the L channel agonist Bay K8644 (25). To directly test the hypothesis that ω-GsTx SIA does not block L channels, we compared the percentage block of I_{Ba} elicited by nimodipine in the absence and presence of ω-GsTx SIA. In the experiment illustrated in Fig. 3, nimodipine blocked 28% of I_{Ba} when applied to a naive cell, and I_{Ba} readily recovered to 96% of base-line levels after removal of nimodipine from the bath. Subseqent application of ω-GsTx SIA blocked 56% of I_{Ba}, after which application of nimodipine elicited an additional 30% block. In three similar experiments, nimodipine blocked 24 ± 5% of total I_{Ba} in the absence of ω-GsTx SIA and 29 ± 1% of total I_{Ba} in the presence of ω-GsTx SIA. Thus, similar components of total I_{Ba} were mediated by dihydropyridine-sensitive Ca^{2+} channels in the absence and presence of ω-GsTx SIA. These results are consistent with the hypothesis that ω-GsTx SIA does not block L-type voltage-gated Ca^{2+} channels.

ω-CmTx MVIIC blocks N-type Ca^{2+} channels in rat CA1 hippocampal neurons and P-type Ca^{2+} channels in rat cerebellar Purkinje neurons (22). In rat cerebellar granule neurons the Q-type component of whole-cell Ca^{2+} channel current was insensitive to dihydropyridines and ω-CgTx GVIA but was blocked by ω-Aga IVA with a K_d of 89 nM; in the same study, Q-type current was also blocked by ω-CmTx MVIIC (8). P channels are blocked by ω-Aga IVA with a K_d of 1–2 nM (7, 8), whereas N channels are selectively blocked by 1 μM ω-CgTx GVIA (6, 13, 14). To pharmacologically identify components of I_{Ba} mediated by the activation of P-, N-, and Q-type Ca^{2+} channels, we measured the cumulative inhibition of I_{Ba} produced by consecutive application of 30 nM ω-Aga IVA, 1 μM ω-CgTx GVIA, and 3 μM ω-CmTx MVIIC.

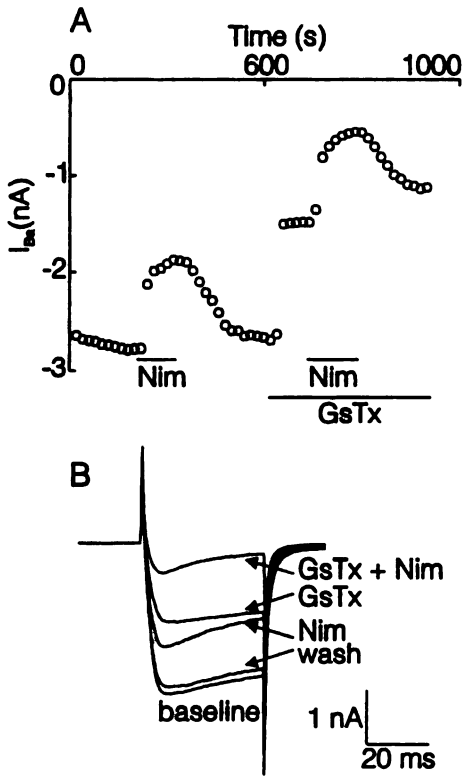

Fig. 3. ω-GsTx SIA does not block L-type Ca^{2+} channels. A, Plot of peak curent versus time, showing that block of I_{Ba} by the L channel blocker nimodipine (*Nim*) (10 μM) is similar before and after block of I_{Ba} by ω-GsTx SIA (*GsTx*) (1 μM). Drugs were applied as indicated (*bars*). B, Current records from the same experiment. *Traces* are averages of three sweeps obtained during each treatment.

The results of these experiments are presented in Fig. 4. The experiment illustrated by the current records in Fig. 4B shows the largest additional block produced by ω-CmTx MVIIC after complete block by ω-Aga IVA and ω-CgTx GVIA. In this experiment, 30 nM ω-Aga IVA blocked 16% of I_{Ba}, and 1 μM ω-CgTx GVIA together with ω-Aga IVA blocked 50% of I_{Ba}. Subsequent application of 3 μM ω-CmTx MVIIC with ω-Aga IVA increased block to 67% of I_{Ba}. ω-CgTx GVIA was not present during exposure of the cell to ω-Aga IVA plus ω-CmTx MVIIC, because ω-CgTx GVIA irreversibly blocks rat N-type Ca^{2+} channels (14). In five similar experiments, summarized in the histogram in Fig. 4A, ω-Aga IVA blocked 22 ± 4% of I_{Ba}, ω-CgTx GVIA combined with ω-Aga IVA blocked 47 ± 5% of I_{Ba}, and ω-CmTx MVIIC combined with ω-Aga IVA blocked 58 ± 5% of I_{Ba}, a significant increase in block over that produced by the combination of ω-Aga IVA and ω-CgTx GVIA ($p < 0.05$).

To address the possibility that additional block of I_{Ba} by ω-CmTx MVIIC in the presence of both ω-Aga IVA and ω-CgTx GVIA was due to incomplete block by either of the latter toxins, we conducted experiments in which cultures were preincubated with 30 nM ω-Aga IVA for at least 15 min before establishment of the whole-cell configuration and were exposed for an additional 5 min to both ω-Aga IVA and ω-CgTx GVIA before application of ω-CmTx MVIIC. In two preincubation experiments, ω-CmTx MVIIC reduced I_{Ba} observed in the presence of ω-Aga IVA and ω-CgTx GVIA by 10% and 21%, confirming that a component of I_{Ba} sensitive to ω-CmTx MVIIC but insensitive to both ω-CgTx GVIA and a P channel-selective concentration of

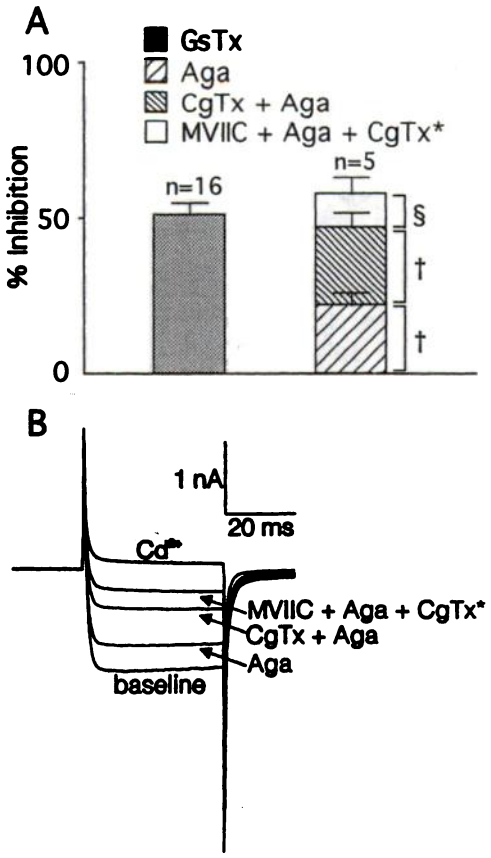

Fig. 4. P-, N-, and Q-type Ca^{2+} channels are present in cultured hippocampal neurons. A, Histogram summarizing and comparing block of I_{Ba} by 1 μM ω-GsTx SIA (*GsTx*) with cumulative block of I_{Ba} by consecutive application of ω-Aga IVA (*Aga*) (30 nM), ω-Aga IVA plus ω-CgTx GVIA (*CgTx*) (1 μM), and ω-Aga IVA plus ω-CmTx MVIIC (*MVIIC*) (3 μM). §, $p < 0.02$; †, $p < 0.001$ (paired Student's *t* test). *, ω-CgTx GVIA had been previously applied, and inhibition by ω-CgTx GVIA was assumed to be irreversible over the time course of this experiment. B, Current records from an experiment such as those summarized in A. *Traces* are the averages of three sweeps obtained after block had reached steady state for each treatment.

ω-Aga IVA is present in cultured hippocampal neurons (data not shown). These experiments demonstrate that P- and N-type Ca^{2+} channels are present in these cells. The additional block by ω-CmTx MVIIC after block by ω-Aga IVA and ω-CgTx GIVA indicates the presence of a component of I_{Ba} that is neither P- nor N-type but is blocked by ω-CmTx MVIIC. It is likely that this component of I_{Ba} is the Q-type current observed under similar conditions in cerebellar granule (8) and CA3 hippocampal (23) neurons. Because ω-CmTx MVIIC blocks P, N, and Q but not L channels and because ω-GsTx SIA blocked a component of I_{Ba} identical to that blocked by ω-CmTx MVIIC and did not block L channels, we conclude that ω-GsTx SIA blocks P-, N-, and Q-type but not L-type voltage-gated Ca^{2+} channels. Consistent with this conclusion, the combination of ω-Aga IVA, ω-CgTx GVIA, and ω-CmTx MVIIC elicited percentage block of I_{Ba} similar to that produced by ω-GsTx SIA alone (Fig. 4A).

ω-Aga IVA blocks P-type Ca^{2+} channels with a K_d of approximately 2 nM. ω-Aga IVA also blocks Q-type Ca^{2+} channels with a K_d of 89 nM (8). Thus, at micromolar concentrations, ω-Aga IVA blocks both P- and Q-type Ca^{2+} channels. To further test the hypothesis that ω-GsTx SIA blocks N, P, and Q channels, we conducted occlusion experiments in which ω-GsTx SIA was tested for the ability to occlude block of I_{Ba} by subsequent application of micromolar ω-Aga IVA and ω-CgTx GVIA applied in combination, and ω-Aga IVA and ω-CgTx GVIA were tested for the ability to occlude block of I_{Ba} by subsequent application of ω-GsTx SIA. These experiments are illustrated in Fig. 5; Fig. 5, A and C, shows plots of peak inward current versus time, and Fig. 5, B and D, shows current records from the same experiments. In the experiment illustrated in Fig. 5, A and B, ω-GsTx blocked 44% of I_{Ba}, and subsequent application of micromolar ω-Aga IVA and ω-CgTx GVIA had no further effect (43% block). In three similar experiments, ω-GsTx blocked 55 ± 7% of I_{Ba}, and addition of ω-Aga IVA together with ω-CgTx GVIA blocked 54 ± 6% of I_{Ba}. Thus, ω-Aga VIA and ω-CgTx GVIA slightly decreased block of I_{Ba}, by 1.7 ± 2.9%, compared with block elicited by ω-GsTx SIA. A similar result was observed when the order of toxin exposure was reversed. In the experiment illustrated in Fig. 5, C and D, the combination of micromolar ω-Aga IVA and ω-CgTx GVIA blocked 36% of I_{Ba}, and subsequent addition of ω-GsTx SIA had no effect (35% block). In three similar experiments, ω-Aga IVA and ω-CgTx GVIA together blocked 54 ± 9% of I_{Ba}, and subsequent exposure to ω-GsTx SIA had no effect (54 ± 10% block). Thus, exposure to ω-GsTx SIA in the presence of ω-Aga IVA and ω-CgTx GVIA produced no change in I_{Ba} (0.0 ± 2.1%). These results support the conclusion that ω-GsTx SIA blocks N-, P-, and Q-type voltage-gated Ca^{2+} channels.

Although ω-GsTx SIA and ω-CmTx MVIIC share Ca^{2+} channel subtype selectivity, we discovered important differences between the toxins during the course of these experiments. First, block by ω-GsTx SIA was faster than block by ω-CmTx MVIIC. The difference in the rates at which ω-GsTx SIA and ω-CmTx MVIIC approach apparent equilibrium may

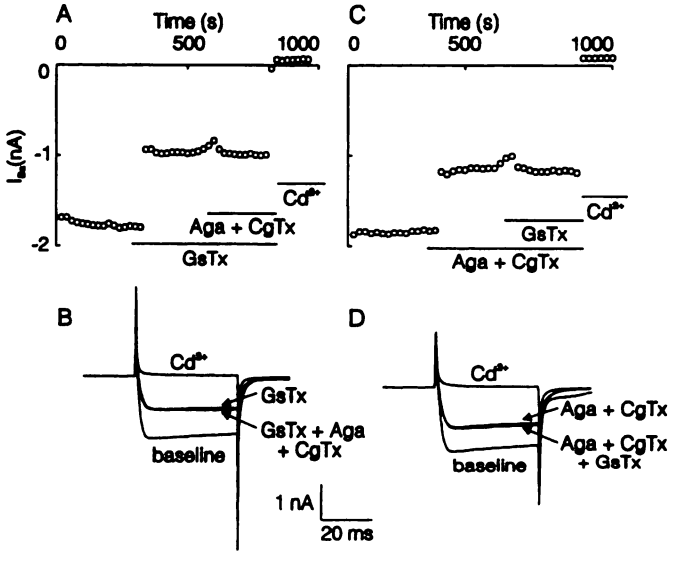

Fig. 5. ω-GsTx SIA blocks N-, P-, and Q-type Ca^{2+} channels. A, Plot of peak current versus time, showing that block by ω-GsTx SIA (*GsTx*) (1 μM) occludes block by the combination of ω-Aga IVA (*Aga*) (1 μM) and ω-CgTx GVIA (*CgTx*) (1 μM). C, Plot of peak current versus time, showing that block by the combination of ω-Aga IVA and ω-CgTx GVIA occludes block by ω-GsTx SIA (same abbreviations and concentrations as in A). Drugs were applied as indicated (*bars*). B and D, Current records from the experiments in A and C, respectively. *Traces* are averages of three sweeps obtained during each treatment. *Scale bars* apply to both sets of currents.

be observed by comparing the plots of peak current versus time in the occlusion experiments illustrated in Fig. 2, A and C. These observations are summarized in Fig. 6, in which the percentage inhibition of peak inward current during the onset of block was normalized to the maximal inhibition achieved for experiments in which naive cells were exposed to either 1 μM ω-GsTx SIA or 3 μM ω-CmTx MVIIC. The point at the origin of the axes (0% of maximal inhibition) corresponds to the last sweep before exposure to toxin, and the points at 20, 40, and 60 sec (the first three points) were recorded before bath exchange was complete. At all points between 80 and 240 sec, where bath exchange was complete and data were available for both toxins, ω-GsTx SIA produced significantly more block than did ω-CmTx MVIIC. After 40 sec, ω-GsTx SIA had achieved 95 ± 1% of its total block, whereas ω-CmTx MVIIC did not reach the same degree of block until 320 sec later. Due to slow bath exchange, early points were collected before toxin concentrations reached reported values; kinetic parameters fully predictive of channel binding affinity are therefore not available from these data, but it is readily apparent that block of I_{Ba} by ω-GsTx SIA is faster than block of the same component of I_{Ba} by ω-CmTx MVIIC.

We also investigated the sensitivity of block by both ω-GsTx SIA and ω-CmTx MVIIC to the external concentration of divalent cations, by repeating the occlusion experiments described in Fig. 2 with 10 mM Ba^{2+}. In the presence of 10 mM Ba^{2+}, 1 μM ω-GsTx SIA blocked 51 ± 14% of I_{Ba}, and subsequent application of 3 μM ω-CmTx MVIIC to the same cells in the presence of ω-GsTx SIA increased inhibition to 57 ± 16% (n = 3). In these experiments, exposure to ω-CmTx MVIIC increased the percentage block of I_{Ba} observed during exposure to ω-GsTx SIA alone by only 5.7 ± 1.7%. Therefore, ω-GsTx SIA produced the same inhibition of I_{Ba} with 10 mM Ba^{2+} as with 5 mM Ba^{2+} and occluded block of I_{Ba} by ω-CmTx MVIIC with 10 mM Ba^{2+} just as with 5 mM Ba^{2+} (Fig. 2). In contrast, block of I_{Ba} by ω-CmTx MVIIC was reduced to 37 ± 8% with 10 mM Ba^{2+}, and subsequent application of ω-GsTx SIA blocked a significant additional fraction of I_{Ba}, increasing the total block to 54 ± 7% ($p < 0.01$, n = 4). In these experiments, block of I_{Ba} by ω-CmTx MVIIC alone was increased by 16 ± 2% upon exposure to ω-GsTx SIA. These data are summarized in the histogram in Fig. 7A and are illustrated in Fig. 7, B and C, in which ω-CmTx MVIIC failed to occlude block of I_{Ba} by ω-GsTx SIA in the presence of 10 mM external Ba^{2+}. This result contrasts with the ability of

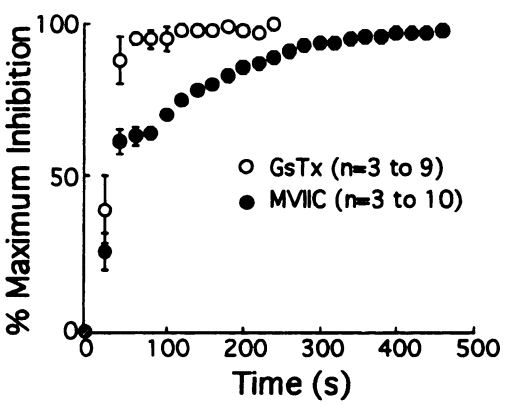

Fig. 6. The onset of block by ω-GsTx SIA is faster than that of block by ω-CmTx MVIIC. At all points after complete bath exchange and for which data were available for both toxins (time points at 80 sec to 240 sec), ω-GsTx SIA (*GsTx*) (1 μM) produced significantly more block than did ω-CmTx MVIIC (*MVIIC*) (3 μM) ($p < 0.001$, analysis of variance and Bonferonni *post hoc* test). Percentage inhibition was normalized to the maximal inhibition attained in each cell. Drugs were applied at time 0. *Error bars* are plotted for all points but are smaller than the symbols at most points. Bath exchange was complete after 60 sec (the third point).

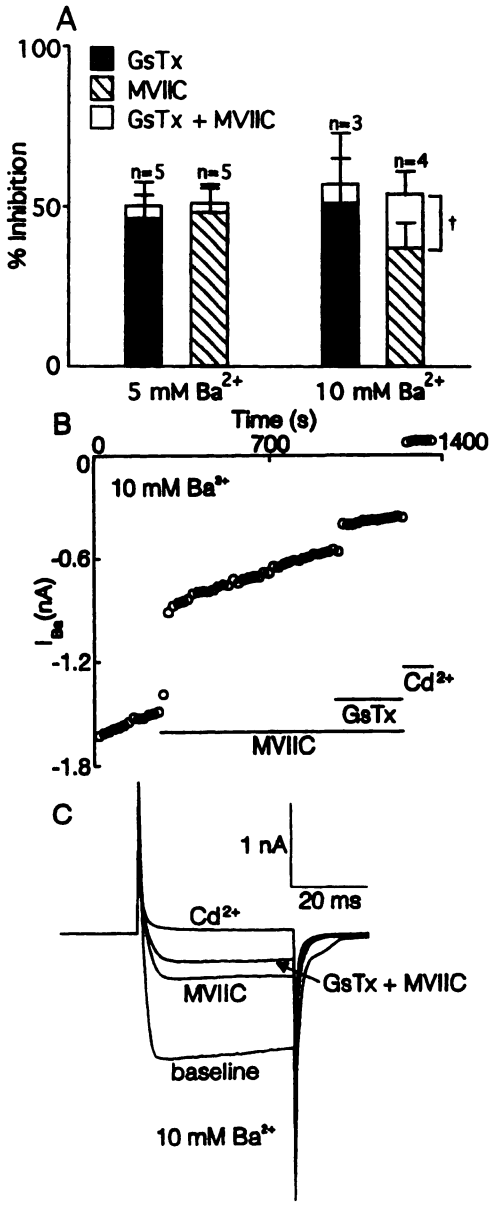

Fig. 7. Block of Ca^{2+} channels by ω-CmTx MVIIC is reduced in the presence of 10 mM Ba^{2+}. A, Histogram summarizing the results of occlusion experiments such as those illustrated in Fig. 2 and in B and C. With 5 mM Ba^{2+}, ω-GsTx SIA (*GsTx*) (1 μM) and ω-CmTx MVIIC (*MVIIC*) (3 μM) were mutually occlusive in their effects on I_{Ba}. With 10 mM Ba^{2+}, ω-GsTx SIA produced block similar to that observed with 5 mM Ba^{2+} and occluded block by ω-CmTx MVIIC, whereas ω-CmTx MVIIC produced less inhibition of I_{Ba} and failed to occlude block by ω-GsTx SIA. Data obtained with 5 mM Ba^{2+} are from occlusion experiments such as those illustrated in Fig. 2. †, $p < 0.01$ (paired Student's t test). B, Plot of peak current versus time for an occlusion experiment in which ω-CmTx MVIIC failed to occlude block of I_{Ba} by ω-GsTx SIA in the presence of 10 mM Ba^{2+}. Drugs were applied as indicated (*bars*). C, Current records from the experiment shown in B. *Current traces* are averages of three sweeps obtained during each treatment.

ω-CmTx MVIIC to occlude block of I_{Ba} by ω-GsTx SIA with 5 mM Ba^{2+}, as illustrated in Fig. 2, C and D. The cause of the decreased block by ω-CmTx MVIIC with 10 mM Ba^{2+} was not apparent. Because the durations of exposure to ω-CmTx MVIIC were similar in the experiments with 5 mM Ba^{2+} (300–520 sec) and 10 mM Ba^{2+} (300–700 sec), decreased block may reflect slower kinetics with the higher external divalent ion concentration. However, with 10 mM Ba^{2+}, ω-GsTx SIA elicited an additional 13% increase in block even after a 700-sec exposure to ω-CmTx MVIIC (Fig. 7, B and C). These results suggest that the ability of ω-CmTx MVIIC to bind to or to block voltage-gated Ca^{2+} channels is diminished when the external concentration of divalent cations is increased, whereas the ability of ω-GsTx SIA to bind to or to block Ca^{2+} channels is relatively unaffected. ω-CmTx MVIIC block of N channels in rat sympathetic neurons is sensitive to the external divalent cation concentration (23).

A previous study suggested that inhibition of Ca^{2+} channels by ω-GsTx SIA was reversible (25). In the present study, this result was confirmed in experiments such as that shown in Fig. 8. In this experiment, 1 μM ω-GsTx SIA produced 84% inhibition of I_{Ba}. Subsequent wash-out of the peptide resulted in recovery of 80% of ω-GsTx SIA-sensitive I_{Ba} within 300 sec. In seven similar experiments, ω-GsTx SIA blocked 54 ± 7% of I_{Ba}, and 61 ± 10% of ω-GsTx SIA-sensitive I_{Ba} recovered within 300 sec after wash-out of the peptide. Recovery ranged from 39 to 100% of the ω-GsTx SIA-sensitive current; thus, ω-GsTx SIA block of I_{Ba} was completely reversible in some cells. The partial recovery observed in some experiments might have resulted from irreversible inhibition of a subtype of voltage-gated Ca^{2+} channels. However, when either 1 μM ω-Aga IVA (n = 3) or 1 μM ω-CgTx (n = 2) GVIA was applied after recovery of I_{Ba} had reached a plateau after wash-out of ω-GsTx SIA, neither toxin produced <21% inhibition of the remaining I_{Ba} (data not shown). These data indicate that ω-GsTx SIA block of N and P channels was reversible, but they do not rule out potentially irreversible inhibition of Q-type Ca^{2+} channels by ω-GsTx SIA.

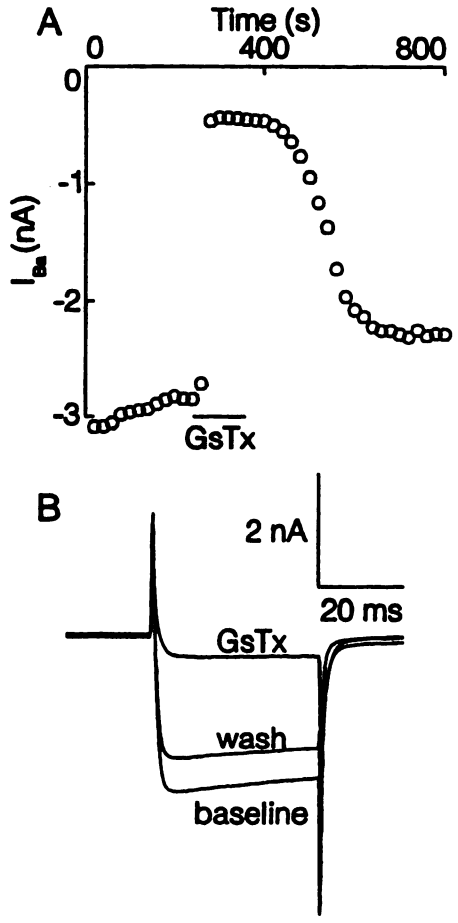

Fig. 8. Block by ω-GsTx SIA is reversible. A, Plot of peak current versus time. ω-GsTx SIA (*GsTx*) (1 μM) was applied as indicated (*bar*). B, Current records from the experiment shown in A. *Current traces* are averages of three sweeps for base-line, the last three sweeps during exposure to ω-GsTx SIA, and three sweeps obtained after recovery had reached steady state.

Discussion

Block of Ca^{2+} channel current by ω-GsTx SIA and by either ω-CmTx MVIIC or the combination of micromolar ω-Aga IVA and ω-CgTx GVIA was mutually occlusive, indicating that each of these treatments blocks the same subset of voltage-gated Ca^{2+} channels present in cultured rat hippocampal neurons. ω-CmTx MVIIC or the combination of micromolar ω-Aga IVA and ω-CgTx GVIA blocks N-, P-, and Q-type (8, 22) but not L-type (22) Ca^{2+} channels. All four Ca^{2+} channel subtypes were present in these cells, and ω-GsTx SIA did not occlude block of L channels by nimodipine. Thus, ω-GsTx SIA blocks N-, P-, and Q-type but not L-type voltage-gated Ca^{2+} channels.

To establish the Ca^{2+} channel subtype specificity of ω-GsTx SIA by occlusion experiments using ω-CmTx MVIIC, both toxins were used at maximally effective concentrations; 1 μM ω-GsTx SIA and 3 μM ω-CmTx MVIIC were determined to be maximal concentrations, because the concentration of either toxin 0.5 log unit higher produced no further inhibition of Ca^{2+} channel current. ω-GsTx SIA inhibits depolarization-evoked neurotransmitter release from rat hippocampal slices with IC_{50} values of 75 nM ([^{3}H]norepinephrine) or 210 nM (D-[^{3}H]aspartate) and inhibits rat synaptosomal Ca^{2+} influx with an IC_{50} of 180 nM (24), consistent with the requirement for 1 μM ω-GsTx SIA to elicit maximal block of voltage-gated Ca^{2+} channels in the present study. ω-CmTx MVIIC inhibits rat synaptosomal Ca^{2+} influx with an IC_{50} of approximately 500 nM (22). Whole-cell recordings in acutely dissociated cerebellar Purkinje neurons suggest that the maximally effective concentration of ω-CmTx MVIIC lies between 1 and 10 μM (22), and inhibition by ω-CmTx MVIIC of I_{Ba} mediated by channels expressed in *Xenopus* oocytes containing cloned α1A+α2/δ+β1 subunits (putatively equivalent to the Q channels) suggests an IC_{50} of <150 nM (27). In acutely dissociated rat sympathetic neurons, ω-CmTx MVIIC blocks N channels with an IC_{50} of 25 nM in the presence of 5 mM Ba^{2+} (23). These results are consistent with the requirement for 3 μM ω-CmTx MVIIC to produce maximal inhibition of voltage-gated Ca^{2+} channels in the present study.

ω-CmTx MVIIC or the combination of micromolar ω-Aga IVA and ω-CgTx GVIA blocks N-, P-, and Q-type Ca^{2+} channels, and in the present study ω-GsTx SIA was mutually occlusive of either treatment in blocking Ca^{2+} channel current. To determine the Ca^{2+} channel subtype selectivity of ω-GsTx SIA, it remained only to determine which of the N, P, and Q channel subtypes were present in the cultured hippocampal neurons used in this study. The K_d for block of P

channels by ω-Aga IVA is 1–2 nM (7, 8), whereas ω-Aga IVA blocks Q-type Ca^{2+} channels in cerebellar granule neurons with a K_d of 89 nM (8). Thus, 30 nM ω-Aga IVA, which should completely block P channels but should not appreciably block Q channels, was used in the present study to pharmacologically identify the component of Ca^{2+} channel current mediated by P channels. Rat N channels are completely, selectively, and irreversibly blocked by low micromolar concentrations of ω-CgTx GVIA (6, 13, 14). Q channels, like N- and P-type but not L-type channels (22), are also blocked by ω-CmTx MVIIC (8). Thus, the presence of P and N channels was detected by consecutive application of selective concentrations of ω-Aga IVA and ω-CgTx GVIA, and additional block of whole-cell Ca^{2+} channel current by ω-CmTx MVIIC beyond the block produced by ω-Aga IVA and ω-CgTx GVIA was interpreted as evidence of the presence of Q channels. Consecutive application of 30 nM ω-Aga IVA, 30 nM ω-Aga IVA plus 1 μM ω-CgTx GVIA, and 30 nM ω-Aga IVA plus 3 μM ω-CmTx MVIIC each produced a fractional increase in the cumulative block of Ca^{2+} channel current. These results demonstrate the presence of P and N channels and suggest the presence of Q channels in cultured rat hippocampal neurons. It is possible, given the relative nonselectivity of ω-CmTx MVIIC, that the non-P/non-N but ω-CmTx MVIIC-sensitive component of Ca^{2+} channel current detected in the present study is not identical to the Q-type current, which exhibited similar pharamcology in cultured cerebellar granule neurons. However, the most likely explanation of the results reported here is that P, N, and Q Ca^{2+} channel subtypes are present in cultured rat hippocampal neurons. Furthermore, the ability of ω-GsTx SIA to occlude block of Ca^{2+} channel current by either ω-CmTx MVIIC or the combination of micromolar ω-Aga IVA and ω-CgTx GVIA, treatments that block P-, N-, and Q-type currents, leads to the conclusion that ω-GsTx SIA blocks all three channel subtypes. We found no evidence that ω-GsTx SIA blocked an ω-CmTx MVIIC-insensitive component of Ca^{2+} channel current, as was suggested in another report that demonstrated an ω-GsTx SIA-sensitive, ω-CmTx MVIIC-insensitive component of synaptosomal glutamate release (28). The apparent conflict in these results might result from methodological differences or might reflect the expression in synaptosomes of a novel, ω-CmTx MVIIC-resistant, Ca^{2+} channel subtype.

These data further suggest that P current comprises 22%, N current comprises 27%, and Q current comprises 11% of the Ca^{2+} channel current elicited in the cultured hippocampal neurons used in this study. Furthermore, block of Ca^{2+} channel current by nimodipine suggests that L current comprises 24% of Ca^{2+} channels present in these cells. These percentages agree reasonably well with the results of studies applying similar methods to acutely dissociated hippocampal neurons, in which 14–26% (CA3-CA1), 21–37% (CA3-CA1), and 19–36% (CA1-CA3) of Ca^{2+} channel current were attributed to P, N, and L channels, respectively (21); 18–25% (CA1-CA3) of Ca^{2+} channel current was not attributable to these channels and thus may have been mediated in part by Q channels. A Q-type component of Ca^{2+} channel current has been reported in acutely dissociated rat hippocampal CA3 neurons (23).

ω-GsTx SIA does not inhibit depolarization-evoked contraction of aorta (24) or occlude dihydropyridine-induced facilitation of whole-cell Ca^{2+} current in rat dorsal root ganglion neurons (25). In the present study, block of Ca^{2+} channel current by ω-GsTx SIA was completely occluded by ω-CmTx MVIIC, which does not block L channels (22). Furthermore, the L channel blocker nimodipine elicited similar block in the presence and absence of ω-GsTx SIA. Thus, ω-GsTx SIA does not block L-type voltage-gated Ca^{2+} channels. Twenty-three percent of I_{Ba} was not blocked by the combination of ω-GsTx SIA and nimodipine but was abolished by Cd^{2+} (n = 11), indicating that it was mediated by activation of voltage-gated Ca^{2+} channels. ω-GsTx SIA and nimodipine together block all four pharmacologically identified, high voltage-activated, Ca^{2+} channels. The demonstration of a Cd^{2+}-sensitive, ω-GsTx SIA-insensitive, nimodipine-insensitive component of Ca^{2+} channel current in the present study suggests the presence of a fifth Ca^{2+} channel subtype, as has been observed in cultured cerebellar granule cells (8, 29).

Although ω-GsTx SIA overlaps with ω-Aga IVA, ω-CgTx GVIA, and ω-CmTx MVIIC in indirect measures of voltage-gated Ca^{2+} channel activity and this study demonstrates that ω-GsTx SIA blocks Ca^{2+} channel current mediated by P, N, and Q channels, binding studies suggest that ω-GsTx SIA does not share a binding site with other toxins on these channel molecules. ω-GsTx SIA displaces neither ^{125}I-ω-CgTx GVIA, ^{125}I-ω-Aga IVA, nor ^{125}I-ω-CmTx MVIIC binding to brain membranes (24). Thus, ω-GsTx SIA defines a novel peptide binding site common to P-, N-, and Q-type channels. The amino acid sequences of these toxins are known, and alignment of the sequences reveals conservation of cysteine residues that are linked by disulfide bonds to form multiple intramolecular loops (24); however, the extreme divergence of the intervening sequences renders structurally relevant interpretation of the present data difficult.

Although ω-GsTx SIA shares Ca^{2+} channel subtype specificity with ω-CmTx MVIIC, important differences between the properties of these toxins are reported here. First, the onset of block by ω-GsTx SIA was considerably faster than that by ω-CmTx MVIIC. Maximal block of Ca^{2+} channel current by ω-GsTx SIA was achieved within the time required to exchange the bath solution, whereas maximal block by ω-CmTx MVIIC required an additional 320 sec of exposure to the toxin. Consistent with these data, the association rate of ω-GsTx SIA is 30-fold faster than that of ω-CmTx MVIIC, as measured by the rate of toxin inhibition of glutamate release from rat cortical synaptosomes (28). Slow onset of P channel block by ω-CmTx MVIIC (τ_{on} of ~15 min) has also been reported in cerebellar Purkinje neurons; however, the onset of N channel block by ω-CmTx MVIIC in sympathetic neurons was rapid (23). The rate of block of cloned $\alpha 1A+\alpha 2/\delta+\beta 1$ (putatively Q-type) channels expressed in *Xenopus* oocytes was slow (τ_{on} of ~420 and ~150 sec at 3 and 5 μM, respectively) and was dependent on the concentration of ω-CmTx MVIIC between 0.15 and 15 μM (27), suggesting that higher concentrations of ω-CmTx MVIIC might have produced faster onset of block in the present study. However, measured IC_{50} values for ω-CmTx MVIIC and ω-GsTx SIA are comparable (discussed above), and ω-CmTx MVIIC was applied at a 3-fold higher concentration than ω-GsTx SIA, suggesting that the kinetic comparison made here merits the conclusion that onset of block by ω-GsTx SIA is faster than block by ω-CmTx MVIIC. Second, block of Ca^{2+} channel current by ω-CmTx MVIIC was more sensitive to elevation of the external divalent cation concentration than was block by ω-GsTx SIA. With 5 mM Ba^{2+}, the two toxins were mutually occlusive. With 10 mM Ba^{2+}, ω-CmTx MVIIC blocked a smaller percentage of

I_{Ba} than with 5 mM Ba^{2+} and failed to occlude block by ω-GsTx SIA, whereas inhibition of I_{Ba} by ω-GsTx SIA and occlusion of block by ω-CmTx MVIIC were unaffected. It is possible that increases in divalent ion concentrations do not decrease efficacy but instead slow the kinetics of block by ω-CmTx MVIIC; however, with 10 mM Ba^{2+}, ω-GsTx SIA elicited a substantial increase in block even after very long exposures to ω-CmTx MVIIC. The observation that block of N channels in rat sympathetic neurons by ω-CmTx MVIIC is weaker with higher external Ba^{2+} concentrations establishes a precedent for these observations (23).

This study also confirms the reversibility of block by ω-GsTx SIA. Within 300 sec of wash-out, 61% of Ca^{2+} channel current inhibited by ω-GsTx SIA recovered, including ω-Aga IVA-sensitive and ω-CgTx GVIA-sensitive components. ω-GsTx SIA inhibition may be completely reversible, because full recovery of ω-GsTx SIA-sensitive current was observed in some experiments. Sensitivity of I_{Ba} to ω-Aga IVA and ω-CgTx GVIA after wash-out of ω-GsTx SIA indicates that block by ω-GsTx SIA of N and P channels is reversible, but this does not address the reversibility of ω-GsTx SIA block of Q channels. The reversibility of ω-CmTx MVIIC was not explored here; however, block by ω-CmTx MVIIC of I_{Ba} mediated by channels expressed in *Xenopus* oocytes containing cloned $\alpha 1A+\alpha 2/\delta+\beta 1$ subunits (putatively Q-type) was reversed by <10% 50 min after wash-out of the toxin (27). Block by ω-CmTx MVIIC of N channels in rat sympathetic neurons is rapidly reversed (τ_{off} of ~15 sec), whereas block by ω-CmTx MVIIC of P channels in rat cerebellar Purkinje neurons is essentially irreversible (23). The reversibility of ω-GsTx SIA renders this toxin a useful tool for studies that require recovery of channel function after inhibition.

As evidence accumulates that multiple, voltage-gated, Ca^{2+} channel subtypes mediate the release of neurotransmitters at different synapses in the brain (for review, see Ref. 11) and that multiple Ca^{2+} channel subtypes may contribute to release of a single neurotransmitter at a given synapse (16, 17), Ca^{2+} channel blockers with broad subtype specificity for the channels that mediate neurotransmitter release will become important research tools for pharmacological inhibition of synaptic transmission. ω-GsTx SIA and ω-CmTx MVIIC share specificity for the Ca^{2+} channel subtypes that have been linked to release of various neurotransmitters, including glutamate. The fast onset, relative insensitivity to divalent cation concentration, and reversibility of inhibition by ω-GsTx SIA, coupled with its ability to block N-, P-, and Q-type Ca^{2+} channels, render this toxin a powerful new tool for the study of voltage-gated Ca^{2+} channels and Ca^{2+} channel-mediated processes.

Acknowledgments

We gratefully acknowledge Dr. Nicholas Saccomano at Pfizer Inc. for kindly providing ω-Aga IVA.

References

1. Katz, B. *The Release of Neurotransmitter Substances*. Liverpool University Press, Liverpool, UK (1969).
2. Levitan, I. B. Modulation of ion channels in neurons and other cells. *Annu. Rev. Neurosci.* **11**:119–136 (1988).
3. Morgan, J. I., and T. Curran. Calcium as a modulator of the immediate-early gene cascade in neurons. *Cell Calcium.* **9**:303–311 (1988).
4. Nowycky, M. C., A. P. Fox, and R. W. Tsien. Three types of neuronal calcium channels with different calcium agonist sensitivity. *Nature (Lond.)* **316**:440–443 (1985).
5. Llinas, R., M. Sugimori, J.-W. Lin, and B. Cherksey. Blocking and isolation of a calcium channel from neurons in mammals and cephalopods utilizing a toxin fraction (FTX) from funnel-web spider poison. *Proc. Natl. Acad. Sci. USA* **86**:1689–1693 (1989).
6. Plummer, M. R., D. E. Logothetis, and P. Hess. Elementary properties and pharmacological sensitivities of calcium channels in mammalian peripheral neurons. *Neuron* **2**:1453–1463 (1989).
7. Mintz, I. M., V. J. Venema, K. M. Swiderek, T. D. Lee, B. P. Bean, and M. E. Adams. P-type calcium channels blocked by the spider toxin ω-Aga-IVA. *Nature (Lond.)* **355**:827–830 (1992).
8. Randall, A., and R. W. Tsien. Pharmacological dissection of multiple types of Ca^{2+} channel currents in rat cerebellar granule neurons. *J. Neurosci.* **15**:2995–3012 (1995).
9. Snutch, P. T., P. J. Leonard, M. M. Gilbert, A. H. Lester, and N. Davidson. Rat brain expresses a heterogeneous family of calcium channels. *Proc. Natl. Acad. Sci. USA* **87**:3391–3395 (1990).
10. Tsien, R. W., P. T. Ellinor, and W. A. Horne. Molecular diversity of voltage-dependent Ca^{2+} channels. *Trends Pharmacol. Sci.* **12**:349–354 (1991).
11. Olivera, B. M., G. P. Miljanich, J. Ramachandran, and M. E. Adams. Calcium channel diversity and neurotransmitter release: the ω-conotoxins and ω-agatoxins. *Annu. Rev. Biochem.* **63**:823–867 (1994).
12. McCleskey, E. W., A. P. Fox, D. Feldman, L. J. Cruz, B. M. Olivera, R. W. Tsien, and D. Yoshikami. Calcium channel blockade by a peptide from *Conus*: specificity and mechanism. *Proc. Natl. Acad. Sci. USA* **84**:4327–4331 (1987).
13. Regan, L. J., D. W. Sah, and B. P. Bean. Ca^{2+} channels in rat central and peripheral neurons: high-threshold current resistant to dihydropyridine blockers and *omega*-conotoxin. *Neuron* **6**:269–280 (1991).
14. Boland, L. M., J. A. Morrill, and B. P. Bean. ω-Conotoxin block of N-type calcium channels in frog and rat sympathetic neurons. *J. Neurosci.* **14**: 5011–5027 (1994).
15. Turner, T. J., M. E. Adams, and K. Dunlap. Multiple Ca^{2+} channel types coexist to regulate synaptosomal neurotransmitter release. *Proc. Natl. Acad. Sci. USA* **90**:9518–9522 (1993).
16. Luebke, J. I., K. Dunlap, and T. J. Turner. Multiple calcium channel types control glutamatergic synaptic transmission in the hippocampus. *Neuron* **11**:895–902 (1993).
17. Wheeler, D. B., A. Randall, and R. W. Tsien. Roles of N-type and Q-type Ca^{2+} channels in supporting hippocampal synaptic transmission. *Science (Washington D. C.)* **264**:107–111 (1994).
18. Regehr, W. G., and I. M. Mintz. Participation of multiple calcium channel types in transmission at single climbing fiber to Purkinje cell synapses. *Neuron* **12**:605–613 (1994).
19. DeFeo, P. A., T. J. Mangano, M. E. Adams, and R. A. Keith. Inhibition of ω-conotoxin GVIA insensitive neurotransmitter release by ω-Aga-IVA. *Pharmacol. Commun.* **1**:273–278 (1992).
20. Turner, T. J., M. E. Adams, and K. Dunlap. Calcium channels coupled to glutamate release identified by ω-Aga-IVA. *Science (Washington D. C.)* **258**:310–313 (1992).
21. Mintz, I. M., M. E. Adams, and B. P. Bean. P-type calcium currents in rat central and peripheral neurons. *Neuron* **9**:85–95 (1992).
22. Hillyard, D. R., V. D. Monje, I. M. Mintz, B. P. Bean, L. Nadasdi, J. Ramachandran, G. Milijanich, A. Azimi-Zoonooz, J. M. McIntosh, L. J. Cruz, J. S. Imperial, and B. M. Olivera. A new *Conus* peptide ligand for mammalian presynaptic Ca^{2+} channels. *Neuron* **9**:69–77 (1992).
23. Swartz, K. D., I. M. Mintz, L. M. Boland, and B. P. Bean. Block of calcium channels in central and peripheral rat neurons by ω-conotoxin-MVIIC. *Soc. Neurosci. Abstr.* **19**:1478 (1993).
24. Lampe, R. A., P. A. DeFeo, M. D. Davison, J. Young, J. L. Herman, R. C. Spreen, M. B. Horn, T. D. Mangano, and R. A. Keith. Isolation and pharmacological characterization of ω-grammotoxin SIA: a novel peptide inhibitor of neuronal voltage-sensitive calcium channel responses. *Mol. Pharmacol.* **44**:451–460 (1993).
25. Piser, T. M., R. A. Lampe, R. A. Keith, and S. A. Thayer. ω-Grammotoxin blocks action-potential-induced Ca^{2+} influx and whole-cell Ca^{2+} current in rat dorsal root ganglion neurons. *Pflügers Arch.* **426**:214–220 (1994).
26. Thayer, S. A., S. N. Murphy, and R. J. Miller. Widespread distribution of dihydropyridine-sensitive calcium channels in the central nervous system. *Mol. Pharmacol.* **30**:505–509 (1986).
27. Sather, W. A., T. Tanabe, J. F. Zhang, Y. Mori, M. E. Adams, and R. W. Tsien. Distinctive biophysical and pharmacological properties of class A (BI) calcium channel $\alpha 1$ subunits. *Neuron* **11**:291–303 (1993).
28. Turner, T. J., R. A. Lampe, and K. Dunlap. Characterization of presynaptic calcium channels with ω-contoxin MVIIC and ω-grammotoxin SIA: role for a resistant calcium channel type in neurosecretion. *Mol. Pharmacol.* **47**: 348–353 (1995).
29. Zhang, J. F., A. D. Randall, P. T. Ellinor, W. A. Horne, W. A. Sather, T. Tanabe, T. L. Schwarz, and R. W. Tsien. Distinctive pharmacology and kinetics of cloned neuronal Ca^{2+} channels and their possible counterparts in mammalian CNS neurons. *Neuropharmacology* **32**:1075–1088 (1993).

Send reprint requests to: S. A. Thayer, Department of Pharmacology, University of Minnesota Medical School, 3–249 Millard Hall, 435 Delaware St. S.E., Minneapolis, MN 55455.